INFECTION AND IMMUNITY, Oct. 1999, p. 5206–5214 Vol. 67, No. 10
0019-9567/99/$04.00+0

Streptococcus parasanguis pepO Encodes an Endopeptidase with Structure and Activity Similar to Those of Enzymes That Modulate Peptide Receptor Signaling in Eukaryotic Cells

EUNICE H. FROELIGER,[1] JOYCE OETJEN,[1] JEFFREY P. BOND,[1,2] AND PAULA FIVES-TAYLOR[1]*

Department of Microbiology and Molecular Genetics, University of Vermont,[1] and Vermont Cancer Center,[2] Burlington, Vermont 05405

Received 27 April 1999/Returned for modification 14 June 1999/Accepted 16 July 1999

Studies in our laboratory have identified two fimbria-associated adhesins, FimA and Fap1, of *Streptococcus parasanguis* FW213. In this study, we isolated and sequenced DNA fragments linked to *fimA* to determine if they contained additional factors associated with adherence, virulence, or survival in the host. An open reading frame just upstream and divergently transcribed from the *fimA* operon was identified and named *pepO*. Northern hybridization indicated that *pepO* is transcribed as a monocistronic message. *pepO* encodes a predicted 631-amino-acid protein with a molecular mass of approximately 70.6 kDa. PepO contains the essential motif HEXXH, typical of many zinc-dependent metalloproteases and metallopeptidases. PepO has significant sequence identity to mammalian metallopeptidases, including endothelin-converting enzyme, which converts a potent vasoconstrictor into its active form, and neutral endopeptidase (NEP), which is involved in terminating the activity of opioid peptides. The opioid peptide metenkephalin is a natural substrate of NEP. Cell extracts of FW213 cleaved metenkephalin at the same site as does NEP, while an extract from an insertionally inactivated *pepO* mutant did not. These results indicate that FW213 *pepO* encodes an enzyme with activity similar to that of known mammalian endopeptidases. Phylogenetic analysis of PepO and its homologues suggests lateral genetic exchange between bacteria and eukaryotes.

Members of the sanguis group of streptococci are highly successful colonizers of both hard and soft surfaces in the human oral cavity and thus represent a significant portion of the indigenous microflora (24). Members of this group of bacteria are important in the development of oral diseases because they are the primary colonizers of newly erupted or freshly cleaned tooth surfaces (7, 35). This colonization initiates the formation of dental plaque, the biofilm associated with caries and periodontal disease. In addition, these organisms are major etiological agents of subacute bacterial endocarditis (5). The successful establishment of streptococci in the host appears to be dependent on the ability of these organisms to adhere to oral as well as to other host surfaces. These surfaces include epithelia, salivary pellicle, platelets, other bacteria in plaque, and extracellular matrix components, particularly fibronectin (22, 28). Adherence is facilitated by multiple adhesins expressed on the surface of the bacterial cell (27, 28).

Adhesion of the oral bacterium *Streptococcus parasanguis* FW213 to an in vitro tooth surface model, saliva-coated hydroxyapatite (SHA), is mediated by peritrichous surface fimbriae (15, 21, 22). The genes encoding two fimbria-associated adhesins, Fap1 and FimA, in FW213 have been identified. The *fap1* gene encodes a high-molecular-weight glycoprotein that is important for adhesion to SHA and appears to be involved in the assembly of fimbriae (56). The *fimA* gene encodes a 36-kDa lipoprotein (20, 23) that is an important virulence factor in *S. parasanguis* endocarditis and appears to promote adherence to fibrin in cardiac vegetations (6). *fimA* is part of an operon that encodes components of an ATP-binding cassette-type membrane transport system. In addition to *fimA*, the *fim* locus includes *fimB* (formerly *orf1*), which encodes an ATP-binding protein, and *fimC* (formerly *orf5*), which encodes a hydrophobic transmembrane protein (20). Homologues of FimA have been identified, and sequence analysis of FimA and its homologues has suggested that this group of proteins belongs to a new subfamily of solute-binding proteins that potentially bind metals (13, 29). Just downstream of the *fimA* operon is the gene *tpx* (formerly *orf3*), which encodes a 20-kDa protein (20) with significant homology to a periplasmic thiol peroxidase (Tpx) of *Escherichia coli* (8). In *E. coli*, Tpx is an enzyme that prevents the formation of reactive oxygen species toxic for many bacteria. Recently, it has been shown that *S. parasanguis* Tpx functions in a similar manner (54). Tpx may play a role of particular importance in the survival of bacteria, such as *S. parasanguis*, that lack catalase.

In this study, we isolated and sequenced DNA fragments upstream of the *fimA* operon in order to identify additional factors that may be associated with adherence to host surfaces, virulence, or survival in the host environment. We identified an open reading frame (ORF) that is divergently transcribed from the *fimA* operon and that encodes an endopeptidase (PepO) with high sequence identity to known bacterial and mammalian endopeptidases.

MATERIALS AND METHODS

Bacterial strains, plasmids, and media. The bacterial strains and plasmids used in this study are listed in Table 1. The wild-type *S. parasanguis* (formerly *S. sanguis*) strain used was FW213 (11). Strain VT1346 *pepO*::Km^r was constructed by insertional inactivation of *pepO* as described below. Streptococcal strains were grown statically in Todd-Hewitt (TH) broth (Difco Laboratories, Detroit, Mich.) in the presence of 5% CO_2 at 37°C. Tetracycline (15 μg/ml) or kanamycin (120 μg/ml) was added as required. *E. coli* JM109 (Promega, Madison, Wis.) served as the host for cloning experiments and for plasmid propagation. Strain LE392 (Promega) served as the host strain for the propagation of recombinant bacteriophage. *E. coli* was grown in Luria-Bertani medium or NZYM medium (40) and, when required for plasmid selection, ampicillin (100 μg/ml), tetracycline (15

* Corresponding author. Mailing address: University of Vermont, Department of Microbiology and Molecular Genetics, Stafford Hall, Burlington, VT 05405. Phone: (802) 656-1121. Fax: (802) 656-8749. E-mail: pfivesta@zoo.uvm.edu.

TABLE 1. Bacterial strains and plasmids used in this study

Strain or plasmid	Relevant characteristic(s)	Source or reference
Strains		
S. parasanguis		
FW213	Wild type	11
VT1346	FW213 *pepO*::*aphA-3*	This study
E. coli		
JM109	Host strain for cloning and plasmid propagation	Promega
LE392	Host strain for propagation of λEMBL3	Promega
Plasmids		
pT7Blue	2.9-kb PCR cloning vector; Ap^r	Novagen
pUC18	2.7-kb cloning vector; Ap^r	New England Biolabs
pVT573	664-bp *Sst*I-*Bgl*II internal fragment of *fimA* ligated into pUC18; Ap^r	20
pVT1198	1.9-kb *Eco*RI fragment containing portions of *pepO* and *fimC* ORFs ligated into pUC18; Ap^r	This study
pVT1378	4.4-kb *Sal*I-*Kpn*I fragment containing *pepO* and 3′ flanking sequences ligated into *Kpn*I-*Sal*I sites of pT7Blue; Ap^r	This study
pVA981	Replicates in *E. coli* but not in streptococci; Tc^r	49
pVT1327	3.5-kb *Pst*I-*Sst*I fragment containing sequences from *pepO* and the *fimA* operon ligated into *Pst*I-*Sst*I sites of pT7Blue; Ap^r	This study
pVT1299	pVT1327 with 1.5-kb *aphA3* gene inserted at *Kpn*I site of *pepO*; Ap^r Km^r	This study
pVT1333	5.0-kb insert from pVT1299 containing disrupted *pepO* gene ligated into pVA981; Km^r Tc^r	This study

μg/ml), or kanamycin (25 μg/ml) was included. Agar was added to a final concentration of 1.5% to prepare solid medium.

The plasmid pT7Blue (Novagen, Madison, Wis.) was used for cloning gel-purified PCR products and for subcloning DNA fragments. A recombinant bacteriophage containing *fimA* and ~4.9 kb of sequence 5′ to the *fimA* operon was isolated from an *S. parasanguis* genomic library as described below, and fragments from the insert were subcloned for sequencing. pVT1198 was constructed by ligating a 1.9-kb *Eco*RI fragment containing 5′ sequences of the *fimA* operon and 5′ sequences of the *pepO* gene (Fig. 1) into pUC18. pVT1378, containing most of the *pepO* gene as well as sequences downstream of *pepO*, was constructed by ligating a 4.4-kb *Kpn*I-*Sal*I restriction fragment into pT7Blue. The plasmid containing an internal fragment of *fimA* was pVT573 (20). pVT1327 was constructed by ligating a 3.5-kb *Pst*I-*Sst*I restriction fragment containing sequences from the *fimA* operon as well as *pepO* sequences (Fig. 1) into pT7Blue. The *pepO* sequences were disrupted in pVT1327 at a unique *Kpn*I site by restriction endonuclease digestion followed by cloning of a 1.5-kb fragment containing *aphA3* into the *Kpn*I site by blunt-end ligation (Fig. 1), generating pVT1299. The vector used to deliver the mutated *pepO* sequences into the *S. parasanguis* chromosome was plasmid pVA981 (55), a 7.1-kb pBR325 derivative carrying a Tc^r determinant active in both *E. coli* and streptococci. The mutated *pepO* sequences were excised from pVT1299 and cloned into the *Eco*RI site of pVA981 by blunt-end ligation, creating pVT1333. Supercoiled pVT1333 was used in allelic replacement experiments to create a *pepO* mutant strain of wild-type FW213.

DNA manipulations. Molecular biology techniques were carried out essentially as described previously (40). Plasmids were isolated from *E. coli* with Mini or Midi column plasmid purification kits (Qiagen, Valencia, Calif.). *S. parasanguis* genomic DNA was isolated with a Puregene DNA isolation kit (Gentra Systems, Inc., Minneapolis, Minn.). Phage DNA was isolated as described previously (40) or with a Qiagen lambda DNA isolation kit. DNA probes used in Southern or plaque hybridization analyses were radiolabeled with [α-^{32}P]dCTP by nick translation with a commercially available kit (Gibco BRL, Grand Island,

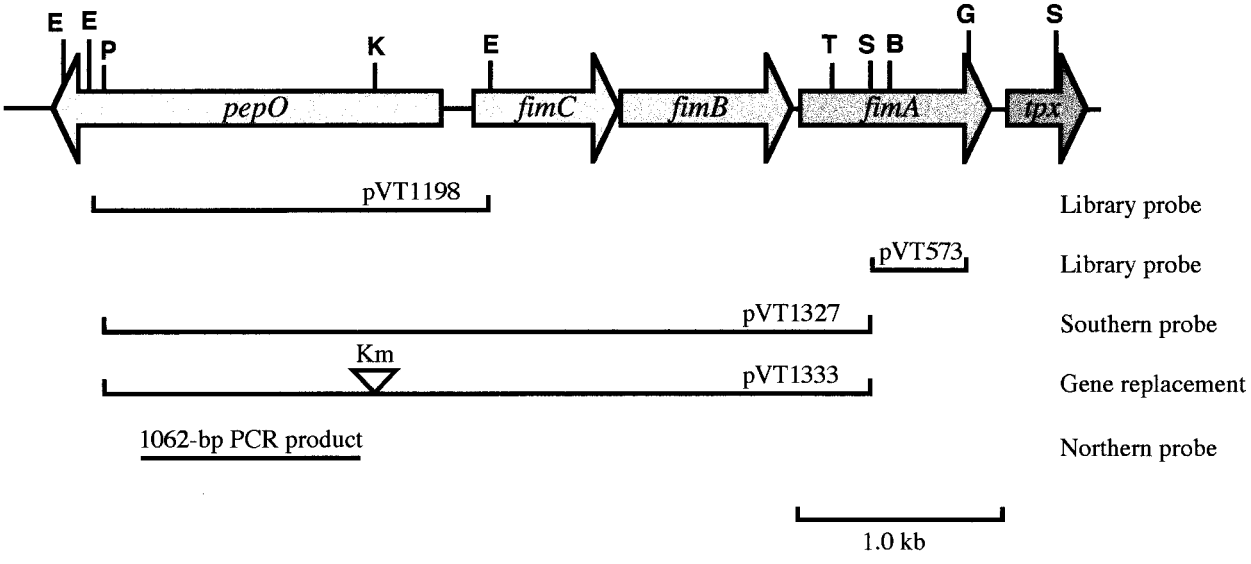

FIG. 1. Physical map of *pepO* and the *fimA* operon region of *S. parasanguis*. The diagram shows a simplified restriction map of a 5.1-kb DNA fragment containing *pepO*, three genes (*fimC*, *fimB*, and *fimC*) of the *fimA* operon, and *tpx*. Arrows indicate the locations and orientations of the ORFs. The lines below the map indicate the sizes and locations of probes and plasmid inserts. The Km^r marker, shown by an open arrowhead, was inserted at the *Kpn*I restriction site of *pepO*. Restriction sites were as follows: B, *Bam*HI; E, *Eco*RI; G, *Bgl*II; K, *Kpn*I; P, *Pst*I; S, *Sal*I; and T, *Sst*I.

TABLE 2. *S. parasanguis* PepO homologues used to construct phylogenetic trees

Protein	Size (amino acids)	% Identity[a]	% Similarity[a]	Organism	GenBank accession no.
PepO	631	100	100	*S. parasanguis*	AF029677
Unknown	631	71	82	*S. pyogenes*	Contig236[b]
Unknown	630	67	78	*S. pneumoniae*	Stp_4114[b]
PepO	627	45	61	*L. lactis*	L18760
PepO	647	37	55	*L. helveticus*	AF019410
Unknown	663	30	47	*Mycobacterium tuberculosis*	AL021928
Unknown	667	29	48	*Mycobacterium leprae*	Z95398
PepO	689	28	47	*Porphyromonas gingivalis*	AB010440
NEP	749	28	43	*Homo sapiens*	X07166
NEP	749	28	43	*Oryctolagus cuniculus*	X05338
NEP	749	28	44	*Mus musculus*	M81591
NEP	749	28	43	*Rattus norvegicus*	M15944
NEP	770	27	44	*Perca flavescens*	AF077612
ECE-1[c]	770	26	43	*H. sapiens*	Z35307
ECE-1	762	26	43	*R. norvegicus*	D29683
ECE-1	754	26	43	*Bos taurus*	Z35306
ECE-1	754	26	42	*Cavia porcellus*	S82653
ECE-2[c]	765	24	42	*H. sapiens*	AB011176
ECE-2	787	23	40	*B. taurus*	U27431
PEX	749	22	40	*H. sapiens*	Y10196
PEX	749	22	40	*M. musculus*	U49908
PEX	749	22	40	*Rattus rattus*	AJ001637

[a] In comparison with *S. parasanguis* PepO, determined by use of BLAST with the BLOSUM62 matrix.
[b] Sequence data from unfinished genome projects.
[c] ECE-1 and ECE-2, isoforms 1 and 2 of ECE, respectively.

N.Y.). Southern and plaque hybridizations were performed as suggested by the membrane manufacturer (Amersham Corp., Arlington Heights, Ill.) and included high-stringency washes.

An *S. parasanguis* FW213 genomic DNA library constructed in λEMBL3 has been described previously (56). The library was transfected into *E. coli* LE392, and recombinant phage carrying *fimA* and sequences 5′ to the *fimA* operon were identified by plaque hybridization analysis (40). pVT573 served as an initial hybridization probe to isolate a recombinant phage carrying *fimA* and sequences 5′ to the *fimA* operon. Subsequently, pVT1198 was used as a probe to obtain a recombinant phage carrying the entire *pepO* gene and sequences downstream from it.

RNA extraction and Northern hybridization analysis. *S. parasanguis* cells were harvested from 10-ml TH broth cultures during mid-logarithmic-phase growth, and the cell pellet was resuspended in water to 200 μl. RNA was isolated from cells with the FastRNA BLUE protocol and a FastPrep instrument according to the manufacturer's (Bio 101, Inc., Vista, Cal.) directions. Cells were processed in the FastPrep instrument at a speed rating of 6 two times for 30 s each time, for a total of 60 s. For Northern analysis, RNA (8 μg) was separated on a 1.2% agarose–0.44 M formaldehyde gel, blotted, and hybridized to an [α-^{32}P]dCTP-labeled DNA probe as previously described (25). A New England Biolabs (Beverly, Mass.) 0.46- to 4.06-kb RNA ladder was used as a molecular weight marker. The probe used was a PCR-amplified 1,062-bp fragment from *pepO* (Fig. 1).

Electrotransformation of *E. coli* and *S. parasanguis*. *E. coli* cells were prepared for electroporation as previously described (4). Cells (50 μl) and approximately 7 μg of DNA were electroporated in a 0.2-cm-gap-size cuvette in a Bio-Rad Gene Pulser set at 2.5 kV, 25 μF, and 200 Ω. Immediately following electroporation, 360 μl of SOC medium (40) was added to the cuvette. Cells were transferred to a 1.5-ml microcentrifuge tube and incubated at 37°C for 1 h. Cells were then spread on Luria-Bertani agar plates supplemented with appropriate antibiotics and incubated overnight at 37°C.

Electrotransformation of *S. parasanguis* cells with plasmid DNA was performed as previously described (19). Immediately following electroporation, 350 μl of recovery medium was added to the cuvette. Cells were transferred to a 1.5-ml microcentrifuge tube and incubated at 37°C in 5% CO_2 for 2 h. Cells were then spread on TH agar plates supplemented with appropriate antibiotics and incubated as described above for 24 to 48 h.

PCR. PCR was performed with a model 9600 thermocycler (Perkin-Elmer Cetus, Norwalk, Conn.) and a GeneAmp PCR reagent kit (Perkin-Elmer Cetus) according to the manufacturer's directions. Genomic DNAs of *S. parasanguis* FW213 and *pepO* allelic replacement mutant VT1346 were amplified with upstream (P1, 5′-TTCTCCCCACAAGACATTC-3′) and downstream (P2A, 5′-GAGTTTGCTCCTTTAC-3′) primers bracketing the *pepO Kpn*I site. The PCR conditions were as follows: one cycle at 94°C for 3 min followed by 35 cycles of 1 min at 94°C, 1 min at 50°C, and 1 min at 72°C. The amplification reaction was completed with an additional cycle of 3 min at 72°C. The PCR amplification products were analyzed by agarose gel electrophoresis.

DNA sequencing and analysis. DNA sequencing was carried out at the Vermont Cancer Center DNA Analysis Facility at the University of Vermont. Nucleotide and protein similarity searches were done with the BLAST programs (1, 2) via the National Center for Biotechnology Information (NCBI) BLAST server (2). Protein similarity searches were conducted with both the NCBI nonredundant protein sequence database and the NCBI database of unfinished genomes. Pairwise and multiple amino acid sequence alignments were obtained with the BLAST and CLUSTAL W (48) programs, respectively, both with the default parameters.

Assay for endopeptidase activity. Endopeptidase activity was assayed by a procedure modified from that of Tan et al. (47). *S. parasanguis* strains were harvested from 500-ml TH broth cultures during late logarithmic growth, washed once with 40 ml of 20 mM potassium phosphate buffer (pH 6.0), and resuspended in 5 ml of cold 20 mM potassium phosphate buffer (pH 6.0). Cells were disrupted with a French press (Aminco, Silver Spring, Md.), with the pressure being maintained at 15,000 lb/in^2. Extracts were obtained from disrupted cells by centrifugation at 17,210 × *g* for 20 min at 4°C. The protein concentration in each cell extract was determined with the bicinchoninic acid protein assay reagent (Pierce, Rockford, Ill.). Reaction mixtures contained 1.25 mM metenkephalin (Tyr-Gly-Gly-Phe-Met; Sigma Chemical Co., St. Louis, Mo.) in 20 mM Tris-HCl at pH 7.0 and 15 μg of cell extract in a total volume of 50 μl. Reaction mixtures were incubated at 30°C, and reactions were stopped by adding 10 μl of 30% acetic acid and cooling the mixtures to 4°C.

Hydrolysis of metenkephalin was detected by thin-layer chromatography (TLC). Samples were centrifuged in a microcentrifuge at 14,000 × *g* for 10 min at 4°C before 10 μl was spotted onto a precoated 0.25-cm-thick silica gel 60 plate (E. Merck AG, Darmstadt, Germany). TLC was performed with *n*-butanol–acetic acid–water (4:1:1 [vol/vol/vol]) as the mobile phase. Ten-microliter samples of 1.25 mM stock solutions of L-glycine, L-phenylalanine, L-methionine, L-tyrosine, and the tripeptide Try-Gly-Gly (Sigma) were spotted onto plates as markers. Silica gels were stained by being sprayed with 0.05% fluorescamine in 99% acetone (Sigma). Amino acids and peptides were visualized in UV light.

Adhesion of *S. parasanguis* to SHA. Preparation of hydroxyapatite beads, clarification of saliva, preparation of SHA beads, and the adhesion assay used have been described previously (15). Data were obtained from two independent one-point adhesion assays (22) performed in triplicate.

Phylogenetic analysis. Numerous *S. parasanguis* PepO amino acid sequence homologues were identified from the BLAST search and analyzed. Several hypothetical nematode proteins and the KELL blood group glycoprotein were not included in the final analysis (see Fig. 6). Inclusion of the nematode and KELL sequences in the analysis did not change the results, but the topologies of the resulting trees were otherwise uncertain. The final data set used to construct phylogenetic trees consisted of the 22 amino acid sequences listed in Table 2.

Multiple amino acid sequence alignments of *S. parasanguis* PepO homologues were edited manually, and positions considered to be aligned with low confidence, including all positions containing gaps, were removed with SEQLAB

(version 9.0; Genetics Computer Group, University of Wisconsin, Madison). The final alignment included 573 sequence positions. Phylogenetic trees were constructed by use of the neighbor-joining algorithm (39) with the programs PROTDIST and NEIGHBOR, both from the PHYLIP program package (16). Phylogenetic trees were also constructed by use of protein parsimony with the PHYLIP and PAUP (Genetics Computer Group) (46) program packages (52). Bootstrap values were calculated with the PHYLIP programs SEQBOOT and CONSENSE and 100 replicates.

Nucleotide sequence accession number. The sequence data for *pepO* have been submitted to the DDBJ, EMBL, and GenBank databases under accession no. AF029677.

RESULTS

Isolation and characterization of the *S. parasanguis pepO* gene. The operon encoding the *S. parasanguis* FW213 fimbria-associated adhesin, *fimA*, was cloned and sequenced previously (18, 19). Initially, pVT573, containing an internal fragment of *fimA* (Fig. 1), was used to screen a genomic *S. parasanguis* phage λEMBL3 library for additional sequences linked to the *fimA* operon. A recombinant phage containing *fimA* and an incomplete upstream ORF was identified. Subsequently, both pVT573 and a 1.9-kb *Eco*RI fragment upstream of *fimA* (Fig. 1) were used to screen the λEMBL3 library again. Of approximately 3,000 plaques screened, 8 that hybridized to both probes were isolated. DNA was prepared from three of the recombinant phage, and restriction enzyme analysis revealed that all three harbored identical inserts. One phage, termed VT1331, was chosen for further investigation. Phage VT1331 contained an insert of approximately 11.0 kb, and Southern hybridization analysis confirmed that the insert contained *fimA* on a 6.0-kb *Eco*RI restriction fragment. A restriction site map of the 11.0-kb insert revealed a 1.9-kb *Eco*RI fragment adjacent to the 6.0-kb *Eco*RI fragment (Fig. 1). Subsequently, this 1.9-kb *Eco*RI fragment, as well as an overlapping 4.4-kb *Sal*I-*Kpn*I fragment, was subcloned from phage VT1331, and the nucleotide sequence of 2.3 kb of DNA was determined.

The product of the ORF upstream of the *fimA* operon displays homology to bacterial and eukaryotic zinc metallopeptidases. Nucleotide sequence analysis of the 2.3-kb region revealed the presence of a single ORF 148 bp upstream and divergently transcribed from the *fimA* operon (Fig. 1). The ORF was comprised of 1,893 nucleotides and was predicted to encode a protein of 631 amino acids and with a molecular mass of approximately 70.6 kDa. No typical signal sequence or regions of hydrophobicity were found in the predicted protein, suggesting that it is a soluble cytoplasmically located protein.

A search of current databases revealed that the predicted protein had significant amino acid sequence homology to a number of bacterial and eukaryotic proteins (Table 2). The highest sequence identity was with hypothetical proteins from *Streptococcus pyogenes* and *Streptococcus pneumoniae* and a partial sequence from *Streptococcus gordonii* (GenBank accession no. L11577) (31). High sequence similarity was also seen with the PepO endopeptidases of *Lactococcus lactis* (34, 53) (Fig. 2) and *Lactobacillus helveticus* (10). The FW213 ORF was designated *pepO* because of the high similarity between its predicted protein product and this latter group of bacterial endopeptidases.

FW213 PepO also showed amino acid similarity to mammalian neutral endopeptidase (NEP; enkephalinase) (9, 12, 32, 33) and to mammalian endothelin-converting enzyme (ECE) (41–43) (Fig. 2). The COOH terminus of the predicted PepO protein contained the sequence HEXXH (Fig. 2), a motif typical of many zinc-dependent metalloproteases and metallopeptidases (26, 36). When a stretch of 80 amino acids surrounding the HEXXH motif was examined, it was determined that *S. parasanguis* PepO had 58% identity and 72% similarity to the equivalent region of human NEP. This same region of *S. parasanguis* PepO also had 53% identity and 70% similarity to human ECE and 76% identity and 82% similarity to *L. lactis* PepO.

The region upstream of the *pepO* coding sequence was found to contain two putative promoter regions with the sequences TTGAAT-19 bp-TATTAA and TTGTAA-17 bp-TATTTT at positions −125 and −39 (with respect to the translational start site), respectively. Within the putative promoter regions was a 32-bp operator-like region consisting of an imperfect repeat with a twofold axis of symmetry. A region with features characteristic of bacterial *rho*-independent transcriptional terminators was found 42 bp downstream from the TAA translational termination codon of *pepO*. This region consisted of a 38-bp imperfect repeat with dyad symmetry followed by a run of five A's. No other ORF of greater than 90 nucleotides was found within 300 bp downstream of the termination codon.

***pepO* is transcribed as a monocistronic message.** Based on DNA sequence analysis, it was reasonable to predict that *pepO* was transcribed as a monocistronic message. Northern hybridization analysis was performed to verify this assumption. A 1,062-bp PCR product (Fig. 1) corresponding to an internal coding region of *pepO* was hybridized to total RNA from *S. parasanguis* FW213 that had been grown in TH broth. Under high-stringency conditions, the probe hybridized to an abundant RNA transcript with an apparent molecular size of approximately 2.1 kb (Fig. 3). A transcript of this size is consistent with the hypothesis that *pepO* is transcribed as a monocistronic mRNA. The *pepO* probe also hybridized to a second, slightly larger and less abundant transcript that is obscured in reproductions of autoradiographs because of its close proximity to the major band. At present, the physiological significance of these two transcripts is unknown.

Construction of an *S. parasanguis pepO* mutant strain. A disrupted allele of *pepO* was constructed by inserting *aphA-3* (50), a gene for kanamycin resistance (Km^r), into the *Kpn*I restriction site of *pepO* (Fig. 1). The mutated allele was cloned into a plasmid unable to replicate in streptococcal cells, and the chromosomal mutation was obtained by the method of allelic replacement (19). The supercoiled plasmid pVT1333, carrying the disrupted *pepO* gene, was transformed into FW213 by electroporation. Transformants arising by allelic replacement were expected to be Km^r and tetracycline sensitive (Tc^s). Therefore, transformants were initially selected for Km^r and then screened for Tc^s. Ten transformants with the expected allelic replacement phenotype were screened by Southern hybridization analysis. The DNA from 9 of 10 transformants gave hybridization patterns indicative of allelic replacement (Fig. 4A). The *pepO* probe hybridized with both 6.0- and 1.9-kb *Eco*RI restriction fragments in the wild-type strain (Fig. 4A, lane 1). The 1.9-kb fragment was absent in the putative *pepO* mutants and replaced by a 3.4-kb fragment (Fig. 4A, lanes 2 and 3). The Southern blot was then stripped and probed with the Km^r determinant *aphA-3* (Fig. 4B). The *aphA-3* probe hybridized with the new 3.4-kb fragment in the *pepO* mutants (Fig. 4B, lanes 2 and 3) but not with fragments in the wild-type strain (lane 1). These data confirm that the shift in size of the fragment from 1.9 to 3.4 kb was due to insertion of the Km^r gene into *pepO*. Proper replacement of the wild-type *pepO* allele with the mutagenized allele was also confirmed by PCR analysis (data not shown). One *pepO* mutant, designated VT1346, was chosen for further study.

The *pepO* mutant adheres to SHA. It is unlikely that PepO acts directly as an adhesin in *S. parasanguis* FW213, but because of the close linkage of *pepO* to the operon encoding the

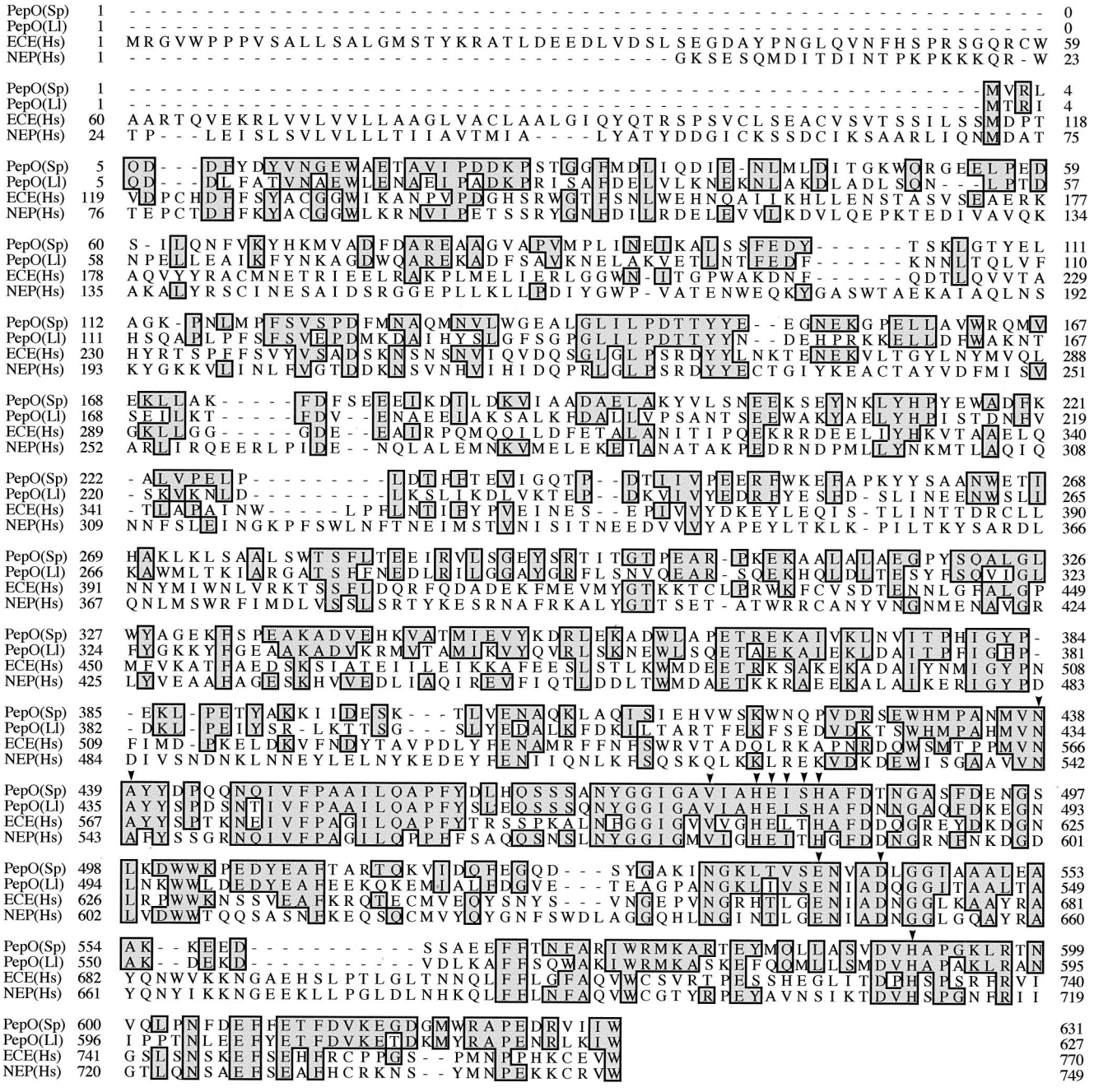

FIG. 2. Sequence of the deduced *S. parasanguis* PepO protein and alignment with related enzymes. Amino acid residues, indicated by the standard one-letter code, are numbered on the left. Highlighted residues were identical to those of the *S. parasanguis* PepO protein. Gaps are indicated by dashes. Arrowheads indicate the HEXXH motif and residues in the mammalian enzymes known to be critical for enzyme activity. The sequences shown are as follows: PepO(Sp), *S. parasanguis* PepO (GenBank accession no. AF029677); PepO(Ll), *L. lactis* PepO (53); ECE(Hs), *H. sapiens* ECE isoform 1 (41); and NEP(Hs), *H. sapiens* NEP (32).

fimbria-associated adhesin, *fimA*, we examined whether PepO plays a role in adhesion. No difference was found between wild-type and mutant strains in an SHA adhesion assay (data not shown), indicating that the inactivation of *pepO* did not affect the ability of *S. parasanguis* cells to adhere to SHA. We also found no obvious differences in growth rate or viability between wild-type and *pepO* mutant cells under standard growth conditions (data not shown).

FW213 PepO has activity similar to that of mammalian NEP. In the human brain, NEP is a major inactivator of endogenous opioid peptides, the enkephalins (38). NEP cleaves substrates at the amino side of hydrophobic amino acids, such as phenylalanine; in the case of the enkephalins, it cleaves at Gly^3-Phe^4. Based on the similarity between *S. parasanguis* PepO and mammalian NEP, we reasoned that *S. parasanguis* FW213 would hydrolyze physiological substrates of NEP but that the *pepO* mutant strain VT1346 would not. Endopeptidase activities of wild-type and *pepO* mutant strains were compared (Fig. 5) with an in vitro assay that included the substrate metenkephalin (Tyr-Gly-Gly-Phe-Met). Endopeptidase activ-

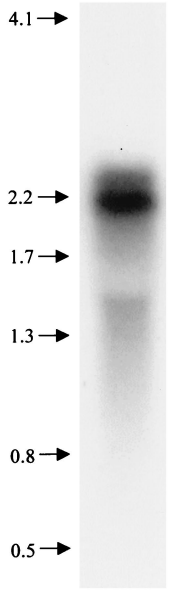

FIG. 3. Northern analysis. RNA (8 μg) was fractionated on a 0.44 M formaldehyde–1.2% agarose gel, blotted, and hybridized to an α-^{32}P-labeled 1,062-bp internal PCR product from *pepO*. Molecular size markers (in kilobases) are shown at the left. The 16S rRNA runs at approximately 1.6 kb.

ity was detected in protein extracts from the wild-type strain but not from the *pepO* mutant strain. Wild-type cell extracts cleaved metenkephalin at the Gly^3-Phe^4 peptide bond, producing the products Tyr-Gly-Gly and Phe-Met (Fig. 5A). These products were not detected when extracts of the *pepO* mutant strain were incubated with the substrate (Fig. 5B). These data indicate that *S. parasanguis* FW213 *pepO* encodes an enzyme with activity similar to those of known mammalian endopeptidases.

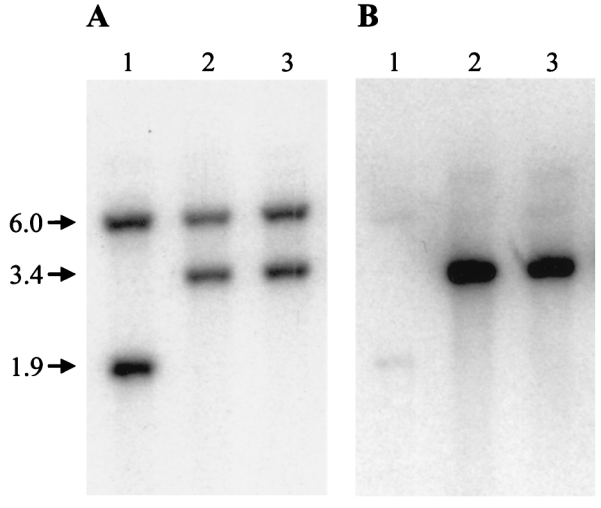

FIG. 4. Southern hybridization analysis of the *pepO* region of wild-type *S. parasanguis* FW213 and two putative *pepO* mutant derivatives. Chromosomal DNA from each strain was digested with *Eco*RI and fractionated on a 0.75% agarose gel. DNA fragments were transferred to Hybond-N$^+$ membranes and hybridized to either pVT1327 (A) or the Km^r determinant *aphA3* (B) that had been α-^{32}P labeled. Lane 1, FW213 DNA; lanes 2 and 3, DNAs from two putative *pepO* mutant derivatives. Sizes in kilobases are noted at the left.

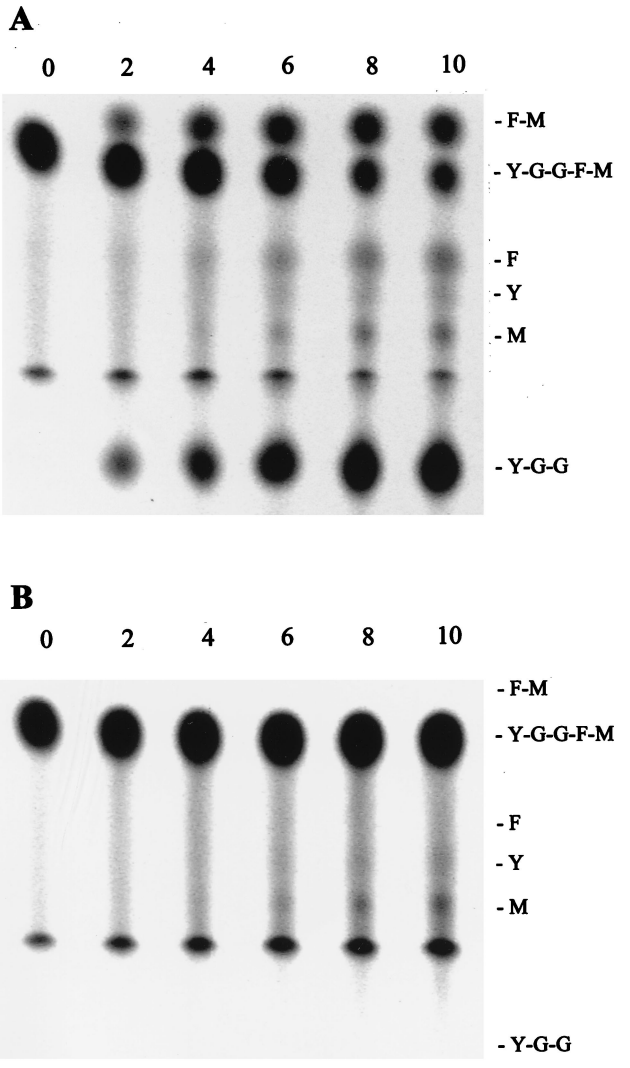

FIG. 5. TLC of metenkephalin hydrolysis by extracts from *S. parasanguis* FW213 and *pepO* mutant VT1346. Protein (15 μg) from FW213 (A) or VT1346 (B) was incubated with 1.25 mM metenkephalin for 0 to 10 min (corresponding to lanes) before termination of the reaction. Endopeptidase activity was detected by TLC. Abbreviations: F-M, phenylalanylmethionine; F, phenylalanine; M, methionine; Y, tyrosine; Y-G-G, tyrosylglycylglycine; Y-G-G-F-M, metenkephalin.

Phylogenetic analysis of PepO and its homologues. Phylogenetic analysis was included in this study because of the striking similarity between bacterial PepO sequences and their eukaryotic homologues. The *S. parasanguis* PepO sequence and 7 bacterial and 14 eukaryotic sequences (Table 2) were aligned and then analyzed by distance methods and by maximum parsimony. A phylogenetic tree (Fig. 6) was constructed from the multiple sequence alignment. Similar results were obtained with different methods of tree construction and with a variety of sequence sets (see Materials and Methods). A clear distinction between eukaryotic and prokaryotic species was seen in 100% of the bootstrap replicates, suggesting that the PepO homologues fall into two monophyletic groups. Within the bacterial branch of the tree, the phylogeny shown was generally consistent with the taxonomic classification given by the NCBI taxonomy browser (47a). What was exceptional about the phylogeny is that PepO homologues were not detected in completely sequenced genomes of organisms representing a broad

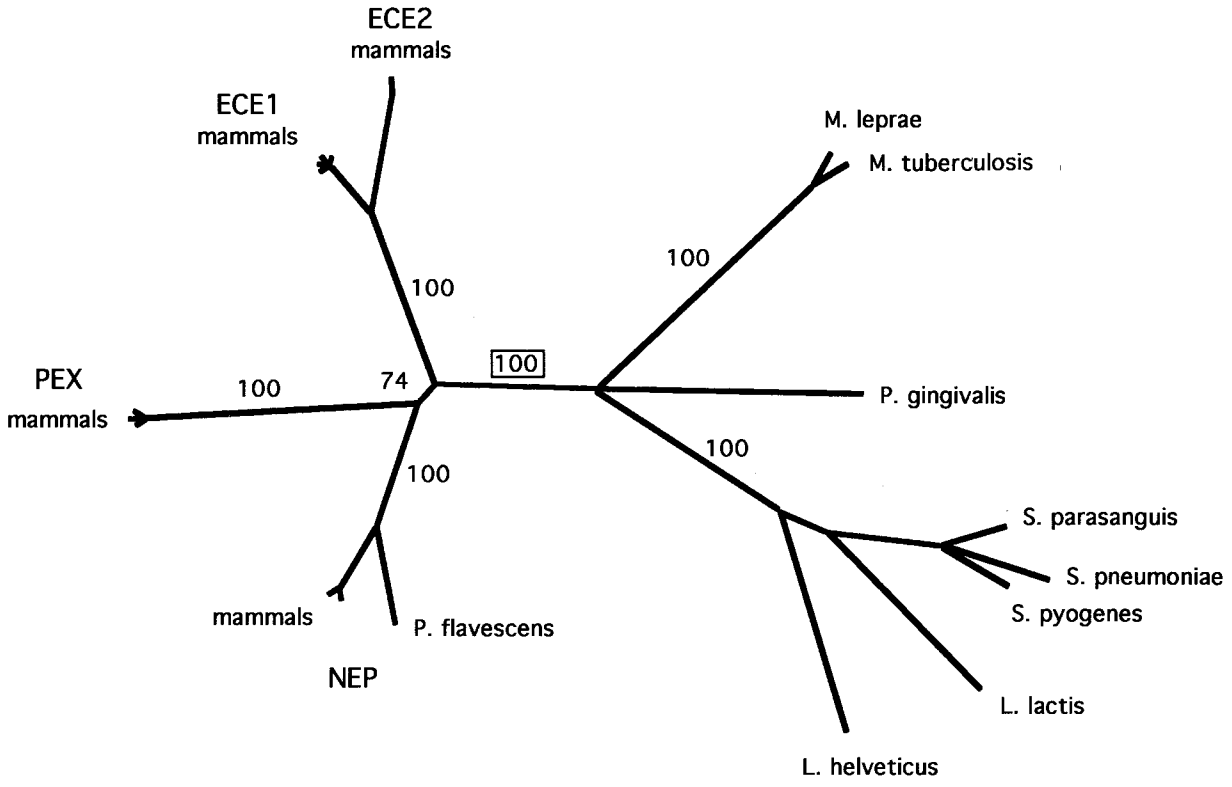

FIG. 6. Phylogenetic tree based on bacterial and eukaryotic PepO sequence homologues. The phylogenetic tree was constructed based on CLUSTAL W alignments of the amino acid sequences listed in Table 2. Numbers on the branches indicate the frequency (percentage) with which the corresponding cluster occurred during bootstrap analysis. ECE-1 and ECE-2, ECE isoforms 1 and 2, respectively; NEP, NEP 24.11; PEX, zinc metallopeptidase homologue (52).

range of taxa. These included archaea, fungi, early branching bacteria (*Aquificales*), proteobacteria, spirochetes, cyanobacteria, chlamydia, mycoplasmas, and *Bacillus subtilis*. These results suggested lateral gene transfer of *pepO* sequences between bacteria and eukaryotes.

DISCUSSION

The purpose of this study was to determine if any factors immediately upstream of the *fimA* operon were associated with adherence or survival within the host. Just 148 bp upstream and divergently transcribed from the *fimA* operon, a 1,893-bp ORF (*pepO*) that encodes a protein with many structural features in common with the M13 (neprilysin) family of metallopeptidases was identified. This family of metallopeptidases includes bacterial members as well as mammalian neuropeptide-processing, immunoregulatory, and peptide hormone-processing zinc metallopeptidases (36). While the role of the bacterial enzymes is uncertain, the mammalian enzymes have been shown to play essential roles in events such as inflammatory response phenomena and in pain and cardiovascular regulation (45, 51, 52).

FW213 PepO contains the essential HEXXH consensus motif typical of this family of peptidases as well as numerous positionally conserved residues known to be critical for the activity of the mammalian enzymes. Some of the most important residues in the active sites of NEP and ECE are included in the HEXXH consensus motif. In mammalian NEP, the two histidines (His^{583} and His^{587}) are zinc-coordinating residues, and the glutamate (Glu^{584}) plays an important role in catalysis (38, 44). In PepO, each of these important residues as well as many other residues surrounding the critical HEXXH consensus motif are positionally conserved (Fig. 2). In addition to the conserved HEXXH motif, FW213 PepO contains other positionally conserved residues known by site-directed mutagenesis to be important in zinc binding, substrate binding, or hydrolytic activity in NEP (Fig. 2). These include (in NEP) an asparagine (Asn^{542}), an alanine (Ala^{543}), and a valine (Val^{580}) that are involved in substrate binding; a third Zn-coordinating ligand (Glu^{646}); an aspartic acid that is critical for hydrolytic activity (Asp^{650}); and a histidine (His^{711}) that may be involved in transition state binding (14, 30, 38, 55).

pepO appears to be transcribed as a monocistronic message. One major transcript and one minor transcript, differing in size by about 200 bases, were consistently detected by Northern hybridization. The 2.1-kb major transcript is within the size range expected from the ORF that is predicted by the *pepO* sequence; the minor transcript is slightly larger. It is possible that these two transcripts are the result of multiple transcription initiation sites or differential RNA processing. The physiological relationship between the two transcripts in *S. parasanguis* is currently unknown. Three distinct NEP mRNAs that differ only in their 5′ noncoding regions have been identified for humans and rats, and data suggest that their expression is regulated developmentally and in a tissue-specific manner (31, 38). The expression of *S. parasanguis pepO* may also be regulated, and we suggest that this regulation may be related to the expression of the *fimA* operon. The tight physical arrangement of *pepO* and the *fimA* operon, as well as the overlapping arrangement of their 5′ regulatory regions, suggests the possible cotranscription of these genes. Further analysis is necessary to determine if specific sequences within the 148-bp region sep-

arating *pepO* and the *fimA* operon are involved in their coregulation.

An investigation of the physiological role of PepO in *S. parasanguis* was initiated by constructing a mutant strain of FW213. Initially, the adhesion and growth properties of the mutant were examined. PepO does not appear to play a role in the adhesion of *S. parasanguis* cells in an in vitro SHA tooth surface model. This finding is not surprising, since it is known that FimA is not required for binding to SHA (17). An important, but as-yet-unanswered question, is whether PepO plays a role in *S. parasanguis* endocarditis, as does FimA (6). In this regard, it is of interest that a putative zinc metallopeptidase, MEP1, which has homology to the M13 family of metallopeptidases (including mammalian NEP and now *S. parasanguis* PepO), has been identified for the highly pathogenic blood-feeding nematode *Haemonchus contortus* (37). *H. contortus* infects the fourth division of the stomach of sheep, goats, and other small ruminants and can induce anemia, weight loss and, in severe cases, death of the animal. The putative zinc metallopeptidase MEP1 is developmentally regulated, with expression being limited to the blood-feeding stages of *H. contortus*. Whereas we found that the disruption of *pepO* did not affect the growth characteristics of FW213 in TH broth under standard conditions, we observed recently that wild-type *S. parasanguis* FW213 forms larger colonies on blood agar plates than the *pepO* mutant. *S. parasanguis* PepO may also play a role during growth in the presence of blood, such as when streptococcal cells gain access to the bloodstream.

Within the M13 family of metallopeptidases, NEP is the prototype and the most thoroughly characterized. The biochemical activity of PepO was examined by testing the ability of wild-type and mutant strains to hydrolyze metenkephalin, a physiological substrate of mammalian NEP. Wild-type cell extracts cleaved metenkephalin at the same site as does NEP, producing the products Tyr-Gly-Gly and Phe-Met. Cell extracts from the *pepO* mutant failed to cleave metenkephalin at the Gly^3-Phe^4 peptide bond. These data indicate that the *pepO* gene in *S. parasanguis* FW213 encodes an enzyme with activity similar to that of NEP. Furthermore, these data emphasize the close correspondence between the active sites of *S. parasanguis* PepO and mammalian NEP. The similarity of PepO to NEP, in terms of conservation of critical amino acid residues and substrate specificity, demonstrates that PepO is a member of the M13 family of metallopeptidases.

Homologues of the PepO endopeptidase occur in many animals but in only a limited group of bacteria, the majority of which are gram positive and pathogenic for humans. We wonder about the origin of this endopeptidase in these diverse organisms. Since the phylogenetic trees constructed in this study are consistent with species trees, it is possible that the ultimate ancestor of PepO and its animal homologues was present in an organism that gave rise to both modern bacteria and eukaryotes. However, PepO sequence homologues were not detected by the BLAST search of completely sequenced genomes representing a broad range of taxa, including those from groups that diverged early. While this finding could be explained by postulating the widespread loss of PepO sequences from this broad range of taxa, it is highly unlikely. A more plausible explanation is that PepO sequences were acquired through horizontal genetic exchange between bacteria and eukaryotes. Given the distribution of PepO homologues that we found, this event probably took place after the divergence of the eubacterial, archaeal, and eukaryotic lineages. Rawlings and Barrett (36) have proposed that the genes for a number of bacterial metallopeptidases were transferred into eukaryotic cells by endosymbiotic organisms that gave rise to organelles. Transfer of PepO probably did not occur by this mechanism, given that PepO sequences have not been found in proteobacteria and recent data indicating that the α-proteobacterium *Rickettsia prowazekii* and mitochondria are specific evolutionary relatives (3). Whereas the direction of genetic transfer cannot be determined from the information currently available, it is clear from the comparison of PepO homologues that the protein, particularly in the region encompassing the active site, is under strong evolutionary constraints.

The PepO homologues play critical roles in eukaryotic physiology, and it is likely that PepO plays an important role in the relatively small group of bacteria that have maintained or acquired similar sequences. Future studies are aimed at elucidating the physiological role of PepO in *S. parasanguis*. PepO may be useful as a model for understanding the regulation of this family of enzymes.

ACKNOWLEDGMENTS

This work was supported by Public Health Service grant R37-DE11000 from the National Institutes of Health. Phylogenetic analysis was performed at the Molecular Modeling Facility of the Vermont Cancer Center, which is supported by the National Cancer Institute and the Lake Champlain Cancer Research Organization.

REFERENCES

1. **Altschul, S. F., W. Gish, W. Miller, E. W. Myers, and J. D. Lipman.** 1990. Basic local alignment search tool. J. Mol. Biol. **215:**403–410.
2. **Altschul, S. F., T. L. Maddem, A. A. Schaffer, J. Zhang, Z. Zhang, W. Miller, and J. D. Lipman.** 1997. Gapped BLAST and PSI-BLAST: a new generation of protein database search programs. Nucleic Acids Res. **25:**3389–3402.
3. **Andersson, S. G. E., A. Zomorodipour, J. O. Andersson, T. Sicheritz-Ponten, U. C. M. Alsmark, R. M. Podowski, A. K. Naslund, A.-S. Eriksson, H. H. Winkler, and C. G. Kurland.** 1998. The genome sequence of *Rickettsia prowazekii* and the origin of mitochondria. Nature **396:**133–140.
4. **Ausubel, F. M., R. Brent, R. E. Kingston, D. D. Moore, J. A. Smith, J. G. Seidman, and K. Struhl (ed.).** 1989. Current protocols in molecular biology. John Wiley & Sons, Inc., New York, N.Y.
5. **Baddour, L. M.** 1994. Virulence factors among gram-positive bacteria in experimental endocarditis. Infect. Immun. **62:**2143–2148.
6. **Burnette-Curley, D., V. Wells, H. Viscount, C. L. Munro, J. C. Fenno, P. Fives-Taylor, and F. L. Macrina.** 1995. FimA, a major virulence factor associated with *Streptococcus parasanguis* endocarditis. Infect. Immun. **63:**4669–4674.
7. **Carlsson, J., M. Grahnen, G. Johnson, and S. Wikner.** 1970. Establishment of *Streptococcus sanguis* in the mouths of infants. Arch. Oral Biol. **15:**1143–1148.
8. **Cha, M.-K., H.-K. Kim, and I.-H. Kim.** 1996. Mutation and mutagenesis of the thiol peroxidase of *Escherichia coli* and a new type of thiol peroxidase family. J. Bacteriol. **178:**5610–5614.
9. **Chen, C., G. Salles, M. F. Seldin, A. E. Kister, E. L. Reinherz, and M. A. Shipp.** 1992. Murine common acute lymphoblastic leukemia antigen (CD10 neutral endopeptidase 24.11): molecular characterization, chromosomal localization, and modeling of the active site. J. Immunol. **148:**2817–2825.
10. **Chen, Y.-S., and J. L. Steele.** 1998. Genetic characterization and physiological role of endopeptidase O from *Lactobacillus helveticus* CNRZ32. Appl. Environ. Microbiol. **64:**3411–3415.
11. **Cole, R. M., G. B. Calandra, E. Huff, and K. M. Nugent.** 1976. Attributes of potential utility in differentiating among 'group H' streptococci or *Streptococcus sanguis*. J. Dent. Res. **55:**A142–153.
12. **Devault, A., C. Lazure, C. Nault, H. Le Moual, N. G. Seidah, M. Chretien, P. Kahn, J. Powell, J. Mallet, A. Beaumont, B. P. Roques, P. Crine, and C. Boileau.** 1987. Amino acid sequence of rabbit kidney neutral endopeptidase 24.11 (enkephalinase) deduced from a complementary DNA. EMBO J. **6:**1317–1322.
13. **Dintilhac, A., and J.-P. Claverys.** 1997. The *adc* locus, which affects competence for genetic transformation in *Streptococcus pneumoniae*, encodes an ABC transporter with a putative lipoprotein homologous to a family of streptococcal adhesins. Res. Microbiol. **148:**119–131.
14. **Dion, N., H. Le Moual, M.-C. Fournie-Zaluski, B. P. Roques, P. Crine, and G. Boileau.** 1995. Evidence that Asn^{542} of neprilysin (EC 4.3.24.11) is involved in binding of the $P_{2'}$ residue of substrates and inhibitors. Biochem. J. **311:**623–627.
15. **Fachon-Kalweit, S., B. L. Elder, and P. Fives-Taylor.** 1985. Antibodies that bind to fimbriae block adhesion of *Streptococcus sanguis* to saliva-coated hydroxyapatite. Infect. Immun. **48:**617–624.
16. **Felsenstein, J.** 1995. PHYLIP (Phylogeny Inference Package) version 3.5c.

Department of Genetics, University of Washington, Seattle.
17. **Fenno, J. C.** 1993. Genetic analysis of a chromosomal locus of *Streptococcus parasanguis* encoding a fimbrial adhesin and membrane transport system. Ph.D. thesis. University of Vermont, Burlington.
18. **Fenno, J. C., D. LeBlanc, and P. Fives-Taylor.** 1989. Nucleotide sequence analysis of a type 1 fimbrial gene of *Streptococcus sanguis* FW213. Infect. Immun. **57:**3527–3533.
19. **Fenno, J. C., A. Shaikh, and P. Fives-Taylor.** 1993. Characterization of allelic replacement in *Streptococcus parasanguis*: transformation and homologous recombination in a 'nontransformable' streptococcus. Gene **130:**81–90.
20. **Fenno, J. C., A. Shaikh, G. Spatafora, and P. Fives-Taylor.** 1995. The *fimA* locus of *Streptococcus parasanguis* encodes an ATP-binding membrane transport system. Mol. Microbiol. **15:**849–863.
21. **Fives-Taylor, P. M.** 1982. Isolation and characterization of a *Streptococcus sanguis* FW213 mutant non-adherent to saliva-coated hydroxyapatite beads, p. 206–209. *In* D. Schlessinger (ed.), Microbiology—1982. American Society for Microbiology, Washington, D.C.
22. **Fives-Taylor, P. M., and D. W. Thompson.** 1985. Surface properties of *Streptococcus sanguis* FW213 mutants nonadherent to saliva-coated hydroxyapatite. Infect. Immun. **47:**752–759.
23. **Fives-Taylor, P. M., F. L. Macrina, T. J. Pritchard, and S. J. Peene.** 1987. Expression of *Streptococcus sanguis* antigens in *Escherichia coli*: cloning of a structural gene for adhesion fimbriae. Infect. Immun. **55:**123–128.
24. **Frandsen, E. V. G., V. Pedrazzoli, and M. Kilian.** 1991. Ecology of viridans streptococci in the oral cavity and pharynx. Oral Microbiol. Immunol. **6:**129–133.
25. **Froeliger, E. H., and P. Fives-Taylor.** 1998. Analysis of adherence-associated gene expression in *Streptococcus parasanguis*: a method for RNA isolation. Methods Cell Sci. **20:**143–151.
26. **Hase, C. C., and R. A. Finkelstein.** 1993. Bacterial extracellular zinc-containing metalloproteases. Microbiol. Rev. **57:**823–837.
27. **Jenkinson, H. F.** 1995. Genetic analysis of adherence by oral streptococci. J. Ind. Microbiol. **15:**186–192.
28. **Jenkinson, H. F., and R. J. Lamont.** 1997. Streptococcal adhesion and colonization. Crit. Rev. Oral Biol. Med. **8:**175–200.
29. **Kolenbrander, P. E., R. N. Andersen, and N. Ganeshkumar.** 1994. Nucleotide sequence of the *Streptococcus gordonii* PK488 coaggregation adhesin gene, *scaA*, and ATP-binding cassette. Infect. Immun. **62:**4469–4480.
30. **Le Moual, H., N. Dion, B. P. Roques, P. Crine, and G. Boileau.** 1994. Asp650 is crucial for catalytic activity of neutral endopeptidase 24-11. Eur. J. Biochem. **221:**475–480.
31. **Li, C., R. M. Booze, and L. B. Hersh.** 1995. Tissue-specific expression of rat neutral endopeptidase (neprilysin) mRNAs. J. Biol. Chem. **270:**5723–5728.
32. **Malfroy, B., J. W. Kuang, P. H. Seeburg, A. J. Mason, and P. R. Schofield.** 1988. Molecular cloning and amino acid sequence of human enkephalinase (neutral endopeptidase). FEBS Lett. **229:**206–210.
33. **Malfroy, B., P. R. Schofield, W. J. Kuang, P. H. Seeburg, A. J. Mason, and W. J. Henzel.** 1987. Molecular cloning and amino acid sequence of rat enkephalinase. Biochem. Biophys. Res. Commun. **144:**59–66.
34. **Mierau, I., P. S. T. Tan, A. J. Haandrikman, J. Kok, K. J. Leenhouts, W. N. Konings, and G. Venema.** 1993. Cloning and sequencing of the gene for a lactococcal endopeptidase, an enzyme with sequence similarity to mammalian enkephalinase. J. Bacteriol. **175:**2087–2096.
35. **Nyvad, B., and M. Kilian.** 1987. Microbiology of the early colonization of human enamel and root surfaces. Scand. J. Dent. Res. **95:**369–380.
36. **Rawlings, N. D., and A. J. Barrett.** 1995. Evolutionary families of metallopeptidases. Methods Enzymol. **248:**183–228.
37. **Redmond, D. L., D. P. Knox, G. Newlands, and W. D. Smith.** 1997. Molecular cloning and characterization of a developmentally regulated putative metallopeptidase present in a host protective extract of *Haemonchus contortus*. Mol. Biochem. Parasitol. **85:**77–87.
38. **Roques, B. P., F. Noble, V. Dauge, M.-C. Fournie-Zaluski, and A. Beaumont.** 1993. Neutral endopeptidase 24.11: structure, inhibition, and experimental and clinical pharmacology. Pharmacol. Rev. **45:**87–146.
39. **Saitou, N., and M. Nei.** 1987. The neighbor-joining method: a new method for reconstructing phylogenetic trees. Mol. Biol. Evol. **4:**406–425.
40. **Sambrook, J., E. F. Fritsch, and T. Maniatis.** 1989. Molecular cloning: a laboratory manual, 2nd ed. Cold Spring Harbor Laboratory Press, Cold Spring Harbor, N.Y.
41. **Schmidt, M., B. Kroger, E. Jacob, H. Seulberger, T. Subkowski, R. Otter, T. Meyer, G. Schmalzing, and H. Hillen.** 1994. Molecular characterization of human and bovine endothelin converting enzyme (ECE-1). FEBS Lett. **356:**238–243.
42. **Shima, H., M. Yamanouchi, K. Omori, M. Sugiura, K. Kawashima, and T. Sato.** 1995. Endothelin-1 production and endothelin converting enzyme expression by guinea pig airway epithelial cells. Biochem. Mol. Biol. Int. **37:**1001–1010.
43. **Shimada, K., M. Takahashi, and K. Tanzawa.** 1994. Cloning and functional expression of endothelin-converting enzyme from rat endothelial cells. J. Biol. Chem. **269:**18275–18278.
44. **Shimada, K., M. Takahashi, A. J. Turner, and K. Tanzawa.** 1996. Rat endothelin converting enzyme-1 forms a dimer through Cys^{412} with a similar catalytic mechanism and a distinct substrate binding mechanism compared with neutral endopeptidase-24.11. Biochem. J. **315:**863–867.
45. **Shipp, M. A., G. B. Stefano, S. N. Switzer, J. D. Griffin, and E. L. Reinherz.** 1991. CD10 (CALLA) neutral endopeptidase 24.11 modulates inflammatory peptide-induced changes in neutrophil morphology, migration, and adhesin proteins and is itself regulated by neutrophil activation. Blood **78:**1834–1841.
46. **Swofford, D. L.** 1997. PAUP (protein alignment using parsimony). Smithsonian Institute, Washington, D.C.
47. **Tan, P. S. T., K. M. Pos, and W. N. Konings.** 1991. Purification and characterization of an endopeptidase from *Lactococcus lactis* subsp. *cremoris* Wg2. Appl. Environ. Microbiol. **57:**3593–3599.
47a. The taxonomy browser. 6 December 1995. [Online.] D. Leipe and V. Sousou. http://www.ncbi.nlm.nih.gov/Taxonomy. [4 March 1999, last date accessed.]
48. **Thompson, J. D., D. G. Higgins, and T. J. Gibson.** 1994. CLUSTAL W: improving the sensitivity of progressive multiple sequence alignment through sequence weighting, position-specific gap penalties and weight matrix choice. Nucleic Acids Res. **22:**4673–4680.
49. **Tobian, J. A., M. L. Cline, and F. L. Macrina.** 1984. Characterization and expression of a cloned tetracycline-resistant determinant from the chromosome of *Streptococcus mutans*. J. Bacteriol. **160:**556–563.
50. **Trieu-Cuot, P., and P. Courvalin.** 1983. Nucleotide sequence of the *Streptococcus faecalis* plasmid gene encoding the 3′5′-aminoglycoside phosphotransferase type III. Gene **23:**331–341.
51. **Turner, A. J., and L. J. Murphy.** 1996. Molecular pharmacology of endothelin converting enzymes. Biochem. Pharmacol. **51:**91–102.
52. **Turner, A. J., and K. Tanzawa.** 1997. Mammalian membrane metallopeptidases: NEP, ECE, Kell, and PEX. FASEB J. **11:**355–364.
53. **Tynkkynen, S., G. Buist, E. Kunji, J. Kok, B. Poolman, G. Venema, and A. Haandrikman.** 1993. Genetic and biochemical characterization of the oligopeptide transport system of *Lactococcus lactis*. J. Bacteriol. **175:**7523–7532.
54. **Van Hoeven, N., G. Spatafora, and P. Fives-Taylor.** 1998. Identification of a putative antioxidant in *Streptococcus parasanguis*. J. Dent. Res. **77:**1214. (Abstract.)
55. **Vijayaraghavan, J., Y.-A. Kim, D. Jackson, M. Orlowski, and L. B. Hersh.** 1990. Use of site-directed mutagenesis to identify valine-573 in the S′1 binding site of rat neutral endopeptidase 24.11 (enkephalinase). Biochemistry **29:**8052–8056.
56. **Wu, H., K. P. Mintz, M. Ladha, and P. M. Fives-Taylor.** 1998. Isolation and characterization of Fap1, a fimbriae-associated adhesin of *Streptococcus parasanguis* FW213. Mol. Microbiol. **28:**487–500.

Editor: J. R. McGhee